Cellular Oncology 29 (2007) 47–58
IOS Press

Chromatin phenotype karyometry can predict recurrence in papillary urothelial neoplasms of low malignant potential

Rodolfo Montironi [a,*], Marina Scarpelli [a], Antonio Lopez-Beltran [b], Roberta Mazzucchelli [a], David Alberts [c], James Ranger-Moore [c], Hubert G. Bartels [c], Peter W. Hamilton [d], Janine Einspahr [c] and Peter H. Bartels [c]

[a] *Section of Pathological Anatomy and Histopathology, Polytechnic University of the Marche Region, Ancona, Italy*
[b] *Unit of Anatomic Pathology, Cordoba University Medical School, Cordoba, Spain*
[c] *College of Public Health, Arizona Cancer Center, University of Arizona, USA*
[d] *The Queen's University, Belfast, Northern Ireland, UK*

Abstract. *Background*: A preceding exploratory study (*J. Clin. Pathol.* **57**(2004), 1201–1207) had shown that a karyometric assessment of nuclei from papillary urothelial neoplasms of low malignant potential (PUNLMP) revealed subtle differences in phenotype which correlated with recurrence of disease. *Aim of the study*: To validate the results from the exploratory study on a larger sample size. *Materials*: 93 karyometric features were analyzed on haematoxylin and eosin-stained sections from 85 cases of PUNLMP. 45 cases were from patients who had a solitary PUNLMP lesion and were disease-free during a follow-up period of at least 8 years. The other 40 were from patients with a unifocal PUNLMP, with one or more recurrences in the follow-up. A combination of the previously defined classification functions together with a new P-index derived classification method was used in an attempt to classify cases and identify a biomarker of recurrence in PUNLMP lesions. *Results*: Validation was pursued by a number of separate approaches. First, the exact procedure from the exploratory study was applied to the large validation set. Second, since the discriminant function 2 of the exploratory study had been based on a small sample size, a new discriminant function was derived. The case classification showed a correct classification of 61% for non-recurrent and 74% for recurrent cases, respectively. Greater success was obtained by applying unsupervised learning technologies to take advantage of phenotypical composition (correct classification of 92%). This approach was validated by dividing the data into training and test sets with $2/3$ of the cases assigned to the training sets, and $1/3$ to the test sets, on a rotating basis, and validation of the classification rate was thus tested on three separate data sets by a leave-k-out process. The average correct classification was 92.8% (training set) and 84.6% (test set). *Conclusions*: Our validation study detected subvisual differences in chromatin organization state between non-recurrent and recurrent PUNLMP, thus allowing a very stable method of predicting recurrence of papillary urothelial neoplasms of low malignant potential by karyometry.

Keywords: Urothelium, papillary urothelial neoplasm of low malignant potential, recurrence

1. Introduction

The 2004 WHO classification of the non-invasive papillary urothelial tumors [31] subdivides the morphologic spectrum of the non-invasive urothelial papillary neoplasia into papilloma, papillary urothelial neoplasm of low malignant potential, low-grade papillary carcinoma, and high-grade papillary carcinoma. It replaces the 1973 WHO system which included urothelial papilloma, and papillary carcinoma of grade 1, grade 2 and grade 3 [24]. PUNLMP basically corresponds to papillary carcinoma of grade 1 [7].

PUNLMP is a clinically important lesion because the patients are at increased risk of developing recurrence. It is not possible to identify those PUNLMP cases that will recur based on conventional histopathologic assessment [2]. A variety of immunohistochemical and molecular markers have been applied to predict

*Corresponding author: Prof. Rodolfo Montironi, Section of Pathological Anatomy and Histopathology, Polytechnic University of the Marche Region (Ancona), School of Medicine, United Hospitals, Via Conca, 71, I-60020 Torrette, Ancona, Italy.
Fax: +39 071 889985; E-mail: r.montironi@univpm.it.

disease recurrence [11,15,27,29]. However, conflicting results have been reported. Recent studies have shown that the evaluation of the nuclear chromatin organization state by karyometry is useful in the identification of patients at risk for recurrence of superficial urothelial carcinoma [22,34].

A preceding exploratory study had shown that a karyometric assessment of nuclei from papillary urothelial neoplasms of low malignant potential revealed subtle differences in phenotype which correlated with recurrence of disease [32]. That study had involved only 20 subjects, ten with recurrence and ten without recurrence. The exploratory study's sample size was too small to run an independent test set, but feature selection had been done with a Bonferroni-correlated significance level of 0.005.

It is the objective of the current study to validate the results from the exploratory study on a larger sample size.

2. Materials and methods

Eighty five cases of PUNLMP were retrieved from the tissue archives of the Section of the Pathological Anatomy and Histopathology, Polytechnic University of the Marche Region (Ancona). This series also included the 20 cases of the exploratory study [32]. 45 were from patients who had a solitary lesion, less than 1 cm in diameter, diagnosed as PUNLMP who were disease-free during a follow-up period of at least 8 years. This group was defined as "*non-recurrent*" (NR). The other 40 were from patients with a unifocal lesion, less than 1 cm in diameter, diagnosed as PUNLMP, one or more recurrences being seen in the follow-up (none of the these cases progressed to a higher grade and/or became invasive) (in most of the cases the first recurrence was seen six months to one year after the removal of the primary tumor). This group was defined as "*recurrent*" (R). The recurrent lesions showed a histological appearance identical to that seen in the first presentation. From this group only the primary or initial tumors were included in the investigation. As far as sex and age of the patients (their mean age was 62.5 years) were concerned, there were no differences when the NR and R groups were compared. The initial tumors and the recurrences were treated by trans-urethral resection. None of the patients received adjuvant therapy, e.g., BCG or intravesical chemotherapy.

All the cases had been fixed in 4% buffered formaldehyde for 24 hours before processing. For the purpose of this study, five-micron thick sections were cut from the paraffin blocks and stained with haematoxylin and eosin (H&E) in the same batch and at the same time.

2.1. Karyometric analysis

Karyometry was carried out at the Arizona Cancer Center, Tucson, AZ, on the fresh H&E stained sections. H&E staining was used so that the results from image analysis could be directly compared and correlated with histopathologic assessment. Bahr [3] and Keenan et al. [18] showed that data derived from H&E and Papanicolaou stains are linearly correlated with those from Feulgen.

The nuclei were recorded on a video-microscope equipped with a 63:1 Zeiss (Zeiss, Oberkochen, Germany) planapochromatic oil immersion objective, N.A. 1.40, and a COHU (San Diego, CA, USA) black and white video camera. An interference filter with a maximum bandpass at 610 nm was used to enhance contrast of the H&E stained sections. The relay optics provided a sampling density of six pixels per linear micrometer. Individual nuclei from the images were edited using an interactive procedure and then filed for feature extraction. Enough fields were recorded to provide 100 nuclei per case. The nuclei were randomly selected from the intermediate and basal layers.

A total of 93 karyometric features were analyzed in this study. These are related to nuclear area, total optical density and chromatin distribution and pattern [4,14,35]. A sample list of features is given in Table 1 (all features are given in relative units of measure; the values in parenthesis refer to an arbitrary code number with which the feature is identified in the computer program).

2.2. Statistical analyses (including a summary of the approach adopted in the preceding exploratory study)

Data analysis in the exploratory study had led to a hierarchic classifier [5,6,9,12,19,32,33]. The same approach was used for the cases recorded here.

The first classification stage was based on a first order linear discriminant function referred to as DF I,1 to discriminate between nuclei from the non-recurrent and from the recurrent cases.

The distribution of discriminant function scores had shown considerable overlap. However, if one chose, as

Table 1
Sample list of features used in the current study (the values in parenthesis refer to an arbitrary code number with which the feature is identified in the computer program)

- Total optical density (Feature No 001)
- Nuclear area (Feature No 002)
- Variance of Optical Density (OD) values (Feature No 006)
- Pixel OD histogram (0.2–0.3 bin) (Feature No 010)
- Run length feature (OD 0.0–0.3, 1–2 pixels) (Feature No 267)
- Run length feature (OD 0.3–0.6, 3–4 pixels) (Feature No 274)
- Percentage of long runs (Feature No 304)
- Gray level non-uniformity (Feature No 305)
- Run length non-uniformity (Feature No 306)
- Percentage of pixels occurring in a run (Feature No 307)
- Mean OD value (Feature No 317)
- OD value 20% above mean OD (Feature No 318)
- Total number of very dark pixels (Feature No 319)
- Total number of medium density pixels (Feature No 320)

a metafeature, a certain percentage of nuclei with high discriminant function scores, a substantial percentage of non-recurrent cases could be classified without error. This "rule 1" was retained for the current validation study, with the same threshold in the discriminant function score distribution, and the same percentage of nuclei expected beyond that threshold.

For the remainder of cases – the great majority of the recurrent cases and the as yet unclassified non-recurrent cases – a second discriminant function, referred to as DF I,2 had been derived. In the exploratory study the case mean scores for the functions DF I,1 and DF I,2 had been submitted to a box classifier [9] which resulted in a correct classification of all NR cases, and of $9/10$ of the R cases.

However, the performance of a box classifier on samples of small size can result in too optimistic an estimate. To derive an estimate of a correct classification rate on a more conservative basis, the data from the exploratory study had been submitted to the non-supervised learning algorithm P-index [5]. Its classification, based on a Bayesian criterion, had resulted in an 85% correct classification rate.

The current validation study followed the above described analytic approach. However, the larger sample size allowed a more detailed analytic assessment. Validation was pursued by a number of separate approaches. First, the exact procedure from the exploratory study was applied to the large validation set. Second, since the DF I,2 function of the exploratory study had been based on a small sample size, a new discriminant function was derived. Next, the validation data set was divided into training and test sets with $2/3$ of the cases assigned to the training sets, and $1/3$ to the test sets, on a rotating basis, and validation of the classification rate was thus tested on three separate data sets by a leave-k-out process. Finally, the larger sample size allowed a different use of non-supervised learning.

2.3. Statistical rationale for multiple discriminant functions

A sequential decision procedure involving two discriminant functions was chosen because it allows a more specific feature selection and hence, better classification success. In this particular case both of these functions were employed as metafeatures which essentially served for dimensionality reduction (Appendix).

3. Results

3.1. Nuclear abnormality and lesion signature

In the enlarged data set of 85 cases, the differences between the NR and the R cases were again found to be very small. The average nuclear abnormality values, computed using as normal reference data set nuclei from normal bladder epithelium recorded in an earlier study [22], are virtually identical for the R and the NR cases (Table 2). The lesion signatures, i.e., the distribution of the nuclear abnormality values, provide clear evidence that the nuclei sampled from the papillary neoplastic lesions in both the non-recurrent and in the recurrent cases deviate significantly from nuclei from normal urothelium. However, the lesion signatures of the non-recurrent and of the recurrent cases are very similar (Fig. 1).

3.2. Discriminant analysis

In the preceding study the discriminant function DF I,1 was based on six features descriptive of nuclear chromatin texture. This function was applied directly to the new data. The score distributions for the NR and the R cases looked virtually the same as those obtained earlier (Fig. 2). The cases in the pilot study thus were representative. The scores for non-recurring cases again extend farther into the high score range.

Figure 3 shows the plot resulting from applying rule 1 (see Materials and methods) from the pilot study to the large data set. On the left side of the threshold in this plot one finds extensive overlap for cases from

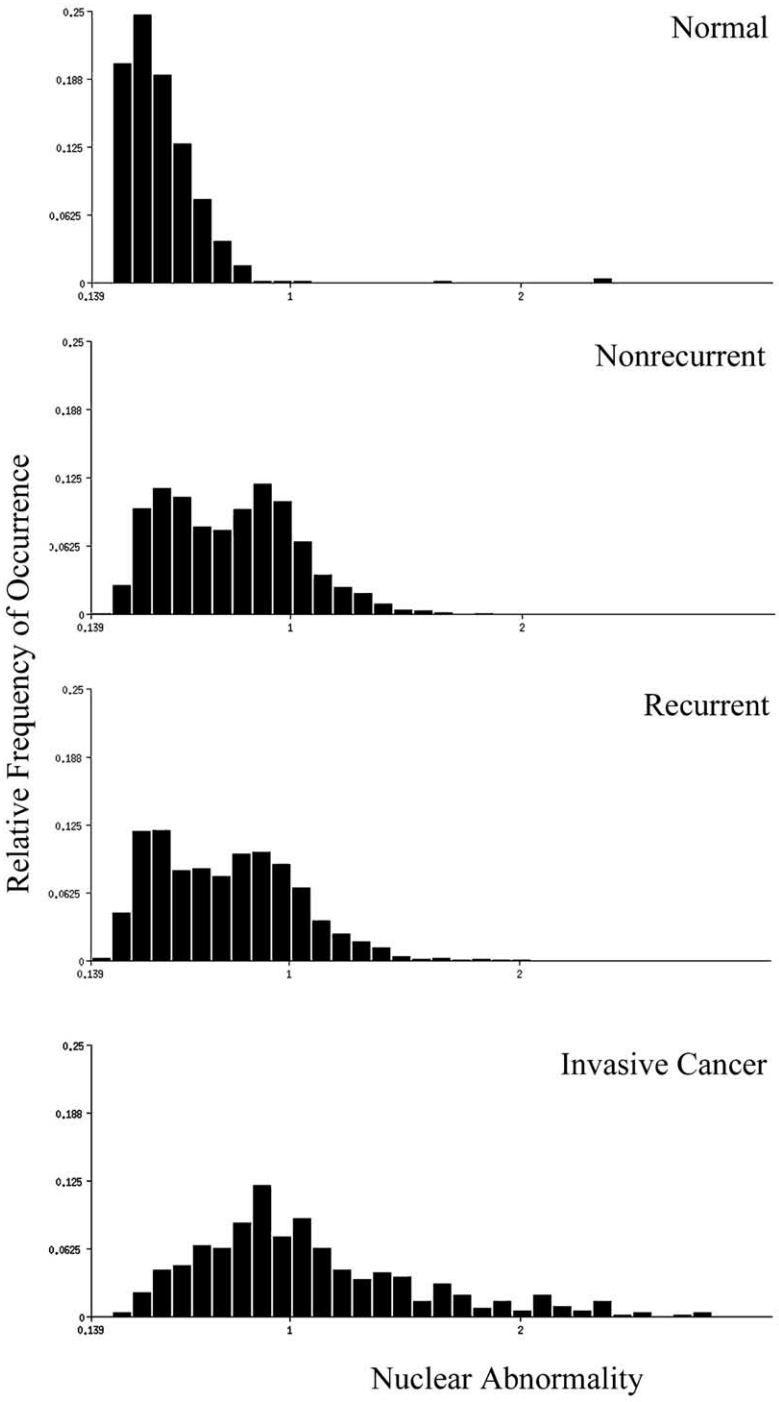

Fig. 1. Lesion signatures for normal, non-recurrent, recurrent, and invasive cancer cases (data on normal urothelium and invasive urothelial carcinoma obtained from a previous study) [20].

both the NR and the R groups. For these cases the pilot study had derived discriminant function DF I,2, as second stage in the hierarchic classifier. This resulted in a classification of $10/10$ of the NR cases, and $8/10$ of the R cases. However, this function was based on only 3 and 4 cases respectively from the NR and R groups. When applied directly to the enlarged data set in the validation study the correct recognition was only about 60%.

A new discriminant function derived from all the cases left after the application of rule 1, combined with the metafeature based on the percentage of nuclei above a certain threshold on the DF I,1 score axis, leads to the plot shown in Fig. 4. There is a correct recognition rate of 82% of the NR cases, and of 73% of the R cases, based on the non-linear decision boundary seen in Fig. 4. The score distribution of this new discriminant function shows a marked shift, and a second order discriminant analysis appeared promising, as seen in Fig. 5.

Table 2

Average nuclear abnormality (data on normal urothelium and invasive urothelial carcinoma obtained from a previous study) [22]

• normal urothelium	0.432
• non-recurrent papillary neoplasm	0.739
• recurrent papillary neoplasm	0.726
• invasive urothelial cancer	1.074

A Kruskal–Wallis (KW) test offered eight features with a p-value <0.005. The second order discriminant algorithm (DF II,1) reduced Wilks Lambda to 0.799. The two distributions of case mean values for the NR and the R data sets are statistically different at a high level of significance. The case classification matrix showed an average correct classification of 61% for NR and 74% for R cases, respectively. This means that there is no gain over the first order discriminant analysis.

It is evident that the nuclei from the NR group and the R group have statistically significantly different chromatin patterns. The discriminant analyses and the bivariate confidence ellipses in Fig. 4 demonstrate this. The case classification is a more difficult problem. With 73% (NR) and 82% (R) correct case classification the results are not deviating from the results obtained in the exploratory study to an unexpected extent, but still, a better yield appeared possible.

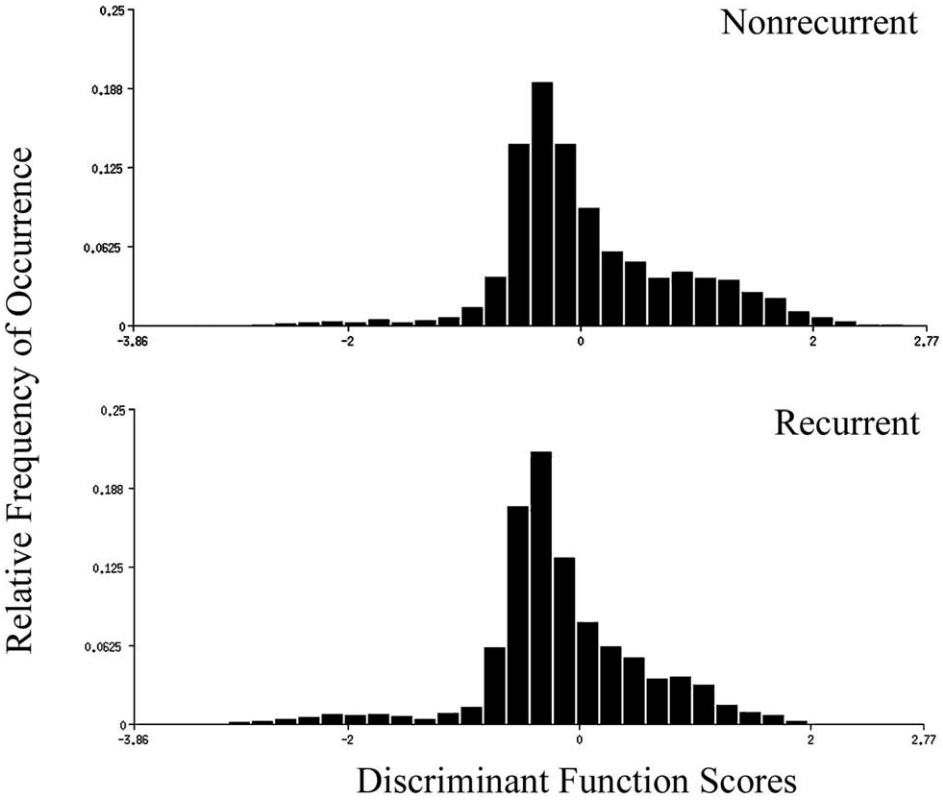

Fig. 2. First order discriminant function score distributions (DF I,1).

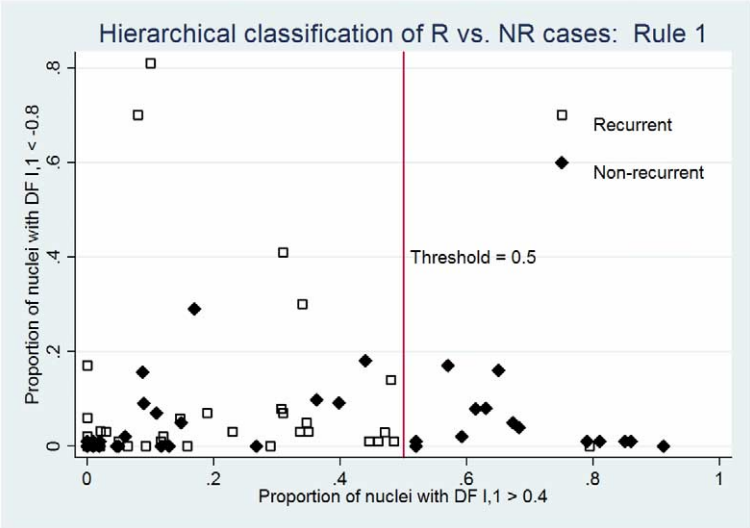

Fig. 3. Illustration of rule 1 in the full data set, whereby cases with the proportion of nuclei having more than 50% of nuclei with DF I,1 $>$ 0.4 are classified as NR.

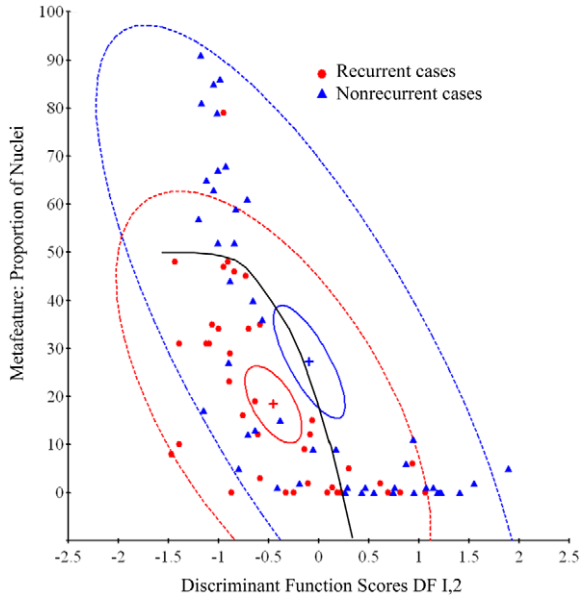

Fig. 4. Proportion of nuclei per case above a fixed threshold vs. discriminant function scores from DF I,2, with a non-linear classification boundary.

3.3. *Classification based on phenotypical composition*

In order to improve classification of cases, an alternative strategy was adopted based on differences in the phenotypical composition of the data sets, if such inhomogeneity could be found. There were 85 cases to start with, and after application of rule 1, 70 cases were left, 39 from the recurrent group, and 31 from the non-recurrent group. The features from the new discriminant function DF I,2 were used, in a first attempt, to explore the phenotypical heterogeneity of the nuclei from these lesions.

Two separate P-index runs were performed, for the NR and the R data sets. In each data set the nuclei were found distributed into four statistically significantly different phenotypes (Fig. 6). These phenotypes closely correspond to each other in the NR and the R data sets. For the two corresponding phenotypes at the one extreme, with, in this instance, negative discriminant function scores indicating the highest deviations from normal, the confidence ellipses overlap completely, they are not statistically different between the NR and the R data sets. For the two corresponding phenotypes appearing at the other extreme range of the feature values, there is an increasing separation of the distributions for the NR and the R data sets (indicated as NR1 and R1). Thus, a classification of cases, based on assignment of nuclei to these two phenotypes appeared possible. Several combinations of features were used to confirm this data structure. Figure 7 shows a plot of a run length feature vs. total optical density, showing the degree of separation between recurrent and non-recurrent cases for one of the four phenotypes depicted in Fig. 6.

Examining only the two corresponding clusters at the high range of the discriminant function score range, 28/39 cases of the R group could be correctly classified, with two errors. Of the NR group, 23/31 cases

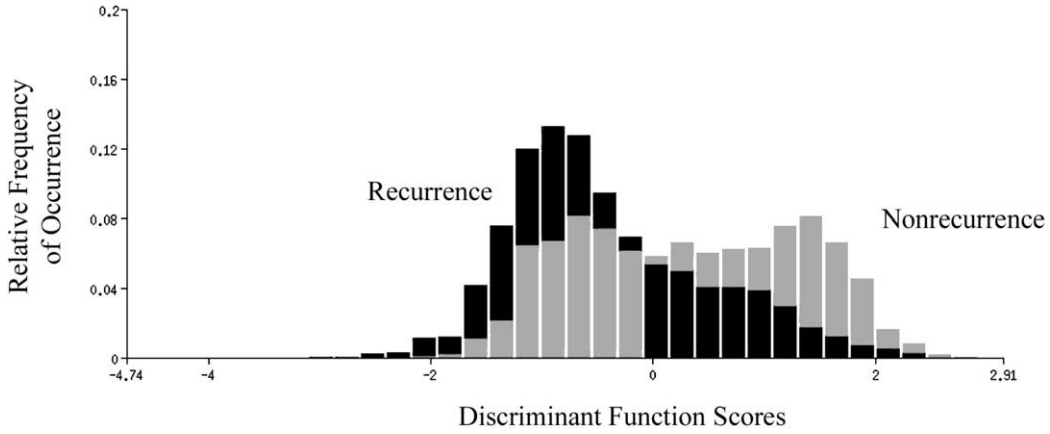

Fig. 5. Distributions of DF I,2 for recurrent and non-recurrent cases. Bins in which the two distributions differ markedly are candidates for the development of a second-order discriminant function.

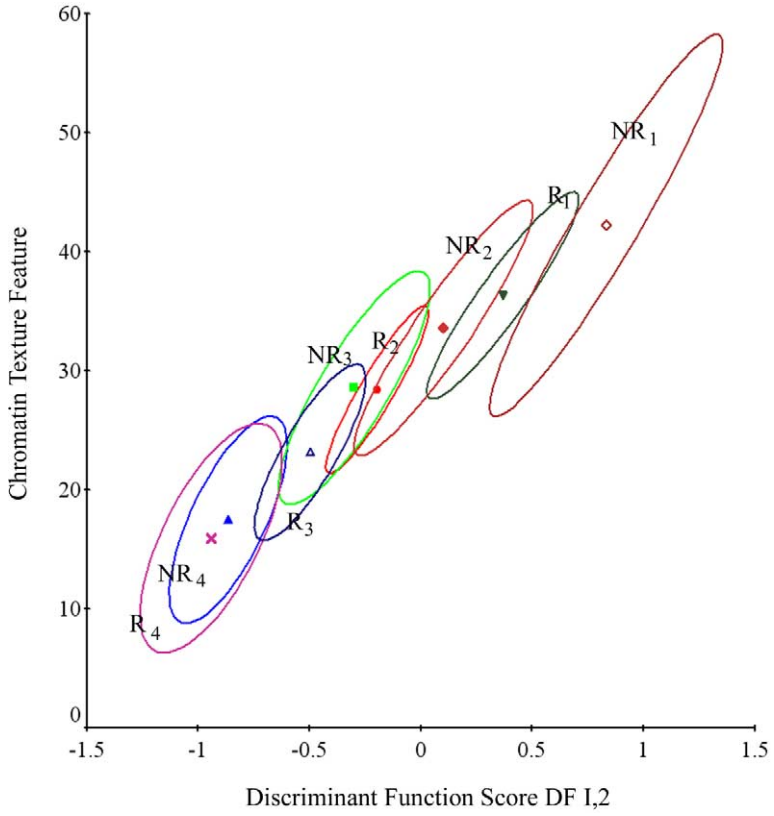

Fig. 6. Distribution of a chromatin texture feature vs. discriminant function score DF I,2, showing four phenotypes each for recurrent and non-recurrent cases.

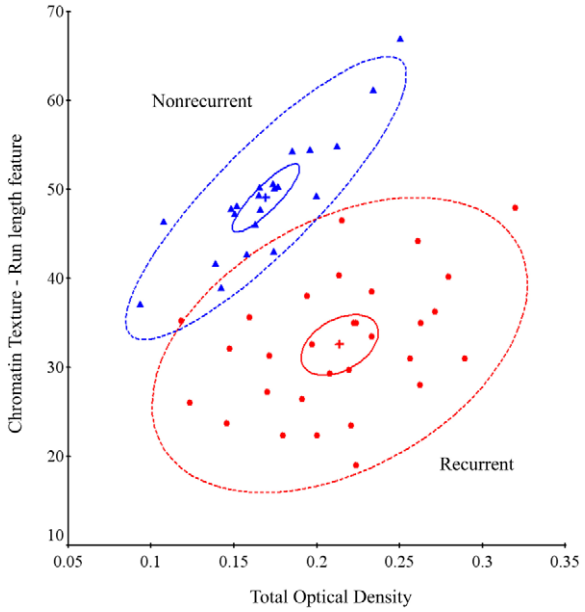

Fig. 7. Plot of a run length feature vs. total optical density, showing the degree of separation between recurrent and non-recurrent cases for one of the four phenotypes depicted in Fig. 6.

were correctly classified, with one error. This step in the hierarchic classification sequence is referred to as rule 2. After eliminating these correctly classified cases, and examining the next corresponding cluster pair (i.e., NR2 and R2), nine more cases of the R group and 4 of the NR group could be correctly assigned, by rule 3. The final accounting for the hierarchic decision sequence of rule 1 and then rules 2 and 3 then came to:

- of 40 R cases, 37 correct, 3 wrong and,
- of 45 NR cases, 41 correct, 1 wrong, 3 not assigned.

Thus, for the total of 85 cases, 91.7% (78/85) were correctly classified into their respective diagnostic groups, with 91.1% (41/45) of the NR cases being correctly classified and 92.5% (37/40) of the R cases correctly classified. These were the results when the entire data set was employed as a test set.

The separation of NR and R cases into two sets of corresponding clusters can be shown for several different sets of features. Figure 7 shows the separation for a feature set consisting of the two features: total optical density and a run length feature. Serving as rule 2 it would provide a correct classification of 29/30 of the submitted R cases, and 22/22 cases of the NR data set, with only a single recurrent case misclassified.

3.4. General validity of the classification success

As a next step in the validation processing, the general validity of the classification success rather than of a given sequence of classification rules, was tested. This was done by randomly dividing the entire data set into three subsets, each formed from 2/3 of cases as a training set, and 1/3 of cases as test set, and rotated three times. Random selection was stratified by recurrence status to maintain proportional balance between R and NR cases. This process would test the performance of independently derived classification rules, and the general validity of each set in the three training set/test set processing sequences.

The following processing sequence was applied. The training set data were used to derive a DF I,1 function. This function was thresholded, and cases with a certain percentage of nuclei with high function scores were identified and removed from further consideration. On the remaining cases a KW test was done and a discriminant function DF I,2 was derived. The features selected by this function were used to run the non-supervised learning algorithm P-index, which was set to form up to four groups. For each of the phenotype subgroups thus formed, the feature mean values of the assigned nuclei were computed, and projected into a display formed by two axes, such as the score values of the discriminant function DF I,2, and one, or two of

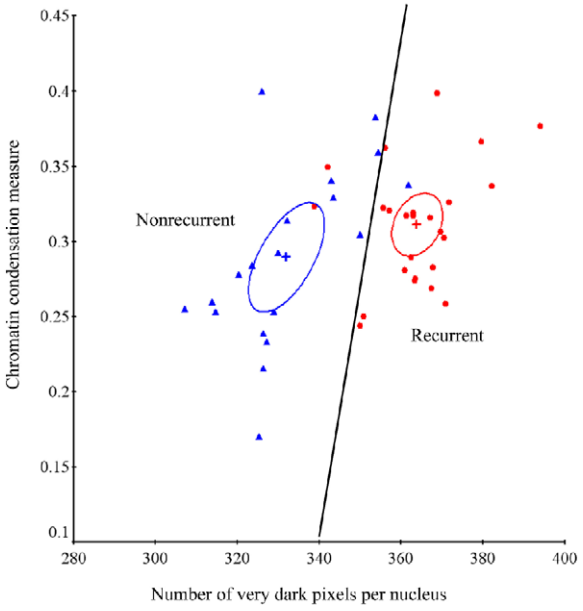

Fig. 8. Plot of chromatin condensation vs. number of very dark pixel per nucleus for recurrent and non-recurrent cases for one of the four phenotypes depicted in Fig. 7.

Table 3
General validity of the classification success

	R correct	NR correct	Overall correct
Training set 1	23/27 85.2%	28/29 96.6%	91.1%
Test set 1	9/13 69.2%	16/16 100%	86.2%
Training set 2	23/27 85.2%	29/30 96.7%	91.2%
Test set 2	7/13 53.8%	15/15 100%	78.6%
Training set 3	24/25 96.0%	29/30 96.7%	96.3%
Test set 3	13/13 100%	12/15 80.0%	89.2%

the chromatin texture features. For the best separated phenotype subgroups of the R and NR data sets, a linear classification boundary was established. Figure 8 shows an example for one of the three validation sets; here, two chromatin texture features had been chosen. The exact same processing sequence was then applied to the test set. This validation processing was repeated for the three training sets and their test sets. However, in each of these three processes an independent feature selection for the DF I,1 and DF I,2 function was carried out, and a different rule 2 was employed. The results for the three validation sets are reported in Table 3. The average correct classification was 92.8% (training set) and 84.6% (test set).

4. Discussion

PUNLMP is a non-invasive papillary urothelial lesion with an orderly arrangement of cells within papillae with minimal architectural abnormalities and minimal nuclear atypia irrespective of cell thickness [31]. In general, the major distinction from papilloma is that in PUNLMP the urothelium is much thicker and/or nuclei are significantly enlarged. The urothelial papilloma, in contrast, has no architectural or cytologic atypia. Mitotic figures are infrequent in PUNLMP, and usually limited to the basal layer. Low-grade papillary urothelial carcinoma is characterized by an overall orderly appearance but with easily recognizable variation of architectural and or cytologic features, even at scanning magnification [21]. Variation in polarity and nuclear size, shape and chromatin texture comprise the minimal but definitive cytological atypia. Mitotic figures are infrequent and usually seen in the lower half [20].

PUNLMP is a clinically important lesion because the patients are at increased risk of developing recurrence. This was documented in 35% and 47% of patients by Holmäng et al. [16] and by Pich et al. [28], respectively. Nevertheless, the prognosis for patients with PUNLMP is excellent. Rarely, these patients may present with tumor progression, i.e., a tumor recurrence with invasion of either the lamina propria or the muscularis propria or with carcinoma *in situ*. In a series of 112 patients described by Cheng et al. [8], only 4 developed invasive urothelial carcinoma, whereas Samaratunga et al. observed a progression rate of 8%, compared to 0% and 13% for papilloma and low-grade papillary carcinoma, respectively [30].

It is not possible to identify those PUNLMP cases that will recur based on conventional histopathologic assessment [28]. A variety of immunohistochemical and molecular markers have been applied to predict disease recurrence [11,15,27,29]. However, conflicting results have been reported. Recent studies have shown that the evaluation of the nuclear chromatin organization state by karyometry is useful in the identification of patients at risk for recurrence of superficial urothelial carcinoma [22,34].

Gschwendtner et al. [13] showed that nuclear texture feature analysis is capable of distinguishing between normal and neoplastic urothelial nuclei, the performance of this approach being superior to DNA ploidy analysis. In a study made by our group [22] we applied a similar technique and we found that karyometry detected an abnormal chromatin pattern and distribution in the normal-looking urothelium adjacent to papillary carcinoma. Such alterations correspond to the so-called malignancy-associated change. Both studies applied such an analysis to cases still classified on the basis of the 1973 WHO scheme and did not investigate the relationship of texture features changes with disease recurrence, even though the existence of some relationship between the chromatin pattern and prognosis was suggested.

Van Velthoven et al. [34] made an investigation on the role of quantitative chromatin pattern analysis in the identification of patients at risk for recurrence. They based their study on the 1973 WHO classification. Patients with either non-invasive (pTa) and lamina propria invasive (pT1) disease (superficial bladder cancer) were considered. They found that discriminant analysis based on chromatin texture features, i.e., related to the level of chromatin distribution and condensation, was more efficient in determining the risk of recurrence than the conventional grading and staging systems.

Our exploratory karyometric study was based on the current grading system (2004 WHO classification), non-invasive PUNLMP lesions only being investigated [13,22,23,34]. Its sample size of 20 provided

80% statistical power to identify classification algorithms as performing statistically significantly better than chance if their true accuracy rates were 80% or higher, a reasonable demand if utility is to be demonstrated. The results from this study went against original expectations: it had been considered unlikely that nuclei collected from biopsies of PUNLMP lesions would provide prognostic information as to which cases might have a recurrence. Similarly to the previous studies [22,34] it has been shown that nuclear chromatin texture features are superior to those concerning the nuclear area and DNA content when those patients who experienced disease recurrence have to be identified.

In the current validation study, karyometry and multivariate analyses detected subvisual differences in chromatin organization state between non-recurrent and recurrent urothelial papillary neoplasm of low malignant potential (the chromatin granules in the latter group are not only darker, but larger), thus providing a valuable biomarker for the prediction of recurrence of papillary urothelial neoplasms of low malignant potential. From the practical point of view, our findings show that a karyometry-based approach could lead to a reduced number of cystoscopies and histological examinations in those patients with a low probability of recurrences. Such patients could be followed up with the evaluation of the urine cytology only.

Little is known about the underlying biological mechanisms responsible for the subvisual differences in chromatin organization state between non-recurrent and recurrent cases. Epigenetic mechanisms such as histone acetylation and DNA methylation, are becoming increasingly recognized as an underlying mechanism in tumour development and are likely to play a major role in determining chromatin pattern. Histone hyperacetylation is associated with a relaxation of chromatin and promotes gene expression whereas DNA hypermethylation, at the level of the gene, results in chromatin condensation and gene silencing. Little work has however examined the association between epigenetic factors and markers such a nuclear karyometry. However, there has recently been a revival in interest regarding the relationship between nuclear architecture, higher order chromatin organization, and the topology of chromosomal territories and their role in regulating gene expression in normal and cancer cells [1,10,17,25,26]. Of particular interest is the identification of chromosomal territories which even in interphase cells occupy specific regions of the nucleus and whose architecture and position seem to be under very close control. This might provide the underlying basis for the global chromatin karyometric changes shown to be of value in the current study.

In conclusion, one has to realize that the differences in chromatin texture which suggest prognostic information have been found to be very subtle indeed. In fact, they are in magnitude and certainty even less pronounced than the changes that have been observed in pre-neoplastic lesions [4,22]. It should be no surprise, therefore, that the procedures to document and validate those changes involve intricate processing steps. As a practical conclusion, this means that in the future studies, one may want to increase the sample size of nuclei beyond 100/case so that a truly representative grouping into phenotypes can be documented. However, this study has demonstrated that chromatin karyometry could be a useful biomarker to predict recurrence in PUNLMP. As with any quantitative approach to tissue analysis, particular using densitometric measurements, standardized sample preparation is extremely important. This would be a prerequisite for the routine use of this technique for predicting recurrence and may make application problematic. Nevertheless, what this study highlights is that specific architectural changes in chromatin organization do exist in lesions that subsequently show recurrence. The underlying molecular basis for this still needs to be understood although it is likely to be associated with epigenetic modifications. It will also be important to investigate other chromatin associated markers that may be stronger and less sensitive to preparation, e.g. measures of DNA methylation and histone acetylation. We are currently investigating in the same series of cases, selected molecular makers, such as cytokeratin 20 and fibroblast growth factor receptor 3, in an attempt to make the statistical analysis less complex and more easily applicable to the routine examination of PUNLMP cases.

Acknowledgement

This study was supported by a grant from the Associazione Italiana per la Ricerca sul Cancro (Marche Region section) (R.M.) and the HPSS Research and Development Office for Northern Ireland (Cancer Recognised Research Group).

Appendix

The first discriminant function (DF I,1) used six features, listed below in order of their relative contributions, with their standardized coefficients.

Feature code	Standardized coefficient	Description
006	0.783	pixel O.D. variance
027	0.584	co-occurrence feature 0–0.3/0.3–0.6 O.D.
267	0.463	run length feature 0–0.3 O.D., 1–2 elements
307	−0.177	run average
303	−0.168	short run emphasis
304	−0.147	long run emphasis

The second discriminant function (DF I,2) used five features:

Feature code	Standardized coefficient	Description
006	−0.918	pixel O.D. variance
306	0.626	run length non-uniformity
272	0.445	run length feature 0–0.3 O.D., 11–12 elements
312	0.252	O.D. heterogeneity measure
001	−0.211	Total optical density

A threshold for DF I,1 was set at DF I,1 = 0.4, and the proportion of cases above that value was used as metafeature. The decision threshold for case classification on this axis was at 50%, as seen on the abscissa in Fig. 3. The same metafeature was used as ordinate in Fig. 4, where the DF I,2 scores serve as abscissa. Figure 4 presents the non-linear decision boundary for case classification.

References

[1] R.L. Adam, R.C. Silva, F.G. Pereira, N.J. Leite, I. Lorand-Metze and K. Metze, The fractal dimension of nuclear chromatin as a prognostic factor in acute precursor B lymphoblastic leukemia, *Cell. Oncol.* **28** (2006), 55–59.

[2] A. Alsheikh, Z. Mohamedali, E. Jones, J. Masterson and C.B. Gilks, Comparison of the WHO/IUSP classification and cytokeratin 20 expression in predicting the behavior of low-grade papillary urothelial tumors, *Mod. Pathol.* **14** (2001), 267–272.

[3] G.F. Bahr, P.H. Bartels, M. Bibbo, M. De Nicolas and G.L. Wied, Evaluation of the Papanicolaou stain for computer assisted cellular pattern recognition, *Acta Cytol.* **17** (1973), 106–112.

[4] P.H. Bartels, R. Montironi, D.G. Bostwick, J. Marshall, D. Thompson, H.G. Bartels and D. Kelley, Karyometry of secretory cell nuclei in high-grade PIN lesions, *Prostate* **48** (2001), 144–155.

[5] P.H. Bartels and G.B. Olson, Computer analysis of lymphocyte images, in: *Methods of Cell Separation*, N. Catsimpoolas, ed., Plenum Press, New York, 1980, pp. 1–99.

[6] E.M. Beale, I. Euclidean cluster analysis, *Bull. Int. Stat. Inst.* **43** (1969), 21–43.

[7] D.G. Bostwick and A. Lopez-Beltran, *Bladder Biopsy interpretation*, United Pathologist Press, New York, 1999.

[8] L. Cheng, R.M. Neumann and D.G. Bostwick, Papillary urothelial neoplasms of low malignant potential. Clinical and biologic implications, *Cancer* **86** (1999), 2102–2108.

[9] W.W. Cooley and P.R. Lohnes, Classification procedures, in: *Multivariate Data Analysis*, W.W. Cooley and P.R. Lohnes, eds, John Wiley, New York, 1971, pp. 262–286.

[10] T. Cremer and C. Cremer, Chromosome territories, nuclear architecture and gene regulation in mammalian cells, *Nature Reviews (Genetics)* **2** (2001), 292–301.

[11] J. Edwards, P. Duncan, J.J. Going, A.D. Watters, K.M. Grigor and J.M. Bartlett, Identification of loci associated with putative recurrence genes in transitional cell carcinoma of the urinary bladder, *J. Pathol.* **196** (2002), 380–385.

[12] J.D. Elashoff, nQuery Advisor® Version 4.0, Los Angeles, CA, 2000.

[13] A. Gschwendtner, Y. Hoffmann-Weltin, G. Mikuz and T. Mairinger, Quantitative assessment of bladder cancer by nuclear texture analysis using automated high-resolution image cytometry, *Mod. Pathol.* **12** (1999), 806–813.

[14] R.M. Haralick, K. Shamugam and I. Dinstein, Textural features for image classification, *IEEE Trans. Man. Cybernet.* **3** (1973), 610–621.

[15] B. Helpap and J. Köllermann, Assessment of basal cell status and proliferative patterns in flat and papillary lesions: a contribution to the new WHO classification of urothelial tumors of the urinary bladder, *Human Pathol.* **31** (2000), 745–750.

[16] S. Holmäng, H. Hedelin, C. Anderström, E. Holmberg, C. Busch and S.L. Johansson, Recurrence and progression in low-grade papillary urothelial neoplasms, *J. Urol.* **162** (1999), 702–707.

[17] A. Huisman, L.S. Ploeger, H.F. Dullens, N. Poulin, W.E. Grizzle and P.J. van Diest, Development of 3D chromatin texture analysis using confocal laser scanning microscopy, *Cell. Oncol.* **27** (2005), 335–345.

[18] S. Keenan, J. Diamond, G. Mccluggage, H. Bharucha, D. Thompson, P.H. Bartels and P.W. Hamilton, Nuclear chromatin texture in the grading of cervical intraepithelial neoplasia (CIN). *Cytometry (Suppl.)* **11** (2002), 116A.

[19] W.H. Kruskal and W.A. Wallis, Use of ranks on one-criterion variance analysis, *J. Am. Stat. Assoc.* **47** (1952), 583–621 (Addendum: **48** (1953), 907–911).

[20] A. Lopez-Beltran and R. Montironi, Non-invasive urothelial neoplasms: according to the most recent WHO classification, *Eur. Urol.* **46** (2004), 170–176.

[21] R. Montironi, A. Lopez-Beltran, R. Mazzucchelli and D.G. Bostwick, Classification and grading of the non-invasive urothelial neoplasms: recent advances and controversies, *J. Clin. Pathol.* **56** (2003), 91–95.

[22] R. Montironi, M. Scarpelli, R. Mazzucchelli, P.W. Hamilton, D. Thompson, J. Ranger-Moore, D.G. Bostwick and P.H. Bartels, Subvisual changes in chromatin organization state are de-

tected by karyometry in the histologically normal urothelium in patients with synchronous papillary carcinoma, *Human Pathol.* **34** (2003), 893–901.

[23] R. Montironi, M. Scarpelli, M. De Nictolis, G.M. Mariuzzi, G. Ansuini and E. Pisani, Comparison of computerized analysis of nuclear DNA changes in uterine cervix dysplasia and in urothelial non-invasive papillary carcinoma, *Pathol. Res. Pract.* **183** (1988), 489–496.

[24] F.K. Mostofi, L.H. Sorbin and H. Torloni, *Histological Typing of Urinary Bladder Tumours. International Classification of Tumours, 19*, World Health Organization, Geneva, 1973.

[25] B. Nielsen and H.E. Danielsen, Prognostic value of adaptive textural features – the effect of standardizing nuclear first-order gray level statistics and mixing information from nuclei having different area, *Cell. Oncol.* **28** (2006), 85–95.

[26] M.C. Osterheld, B.S. Andrejevic, L. Caron, R. Braunschweig, G. Dorta, H. Bouzourene and A. Mihaescu, Digital image DNA cytometry: a useful tool for the evaluation of malignancy in biliary strictures, *Cell. Oncol.* **27** (2005), 255–260.

[27] A. Pich, L. Chiusa, A. Formiconi, D. Galliano, P. Bortolin and R. Navone, Biologic differences between non-invasive papillary urothelial neoplasms of low malignant potential and Low-Grade (Grade 1) papillary carcinomas of the bladder, *Am. J. Surg. Pathol.* **25** (2001), 1528–1533.

[28] A. Pich, L. Chiusa, A. Formiconi, D. Galliano, P. Bortolin, A. Comino and R. Navone, Proliferative activity is the most significant predictor of recurrence in non-invasive papillary urothelial neoplasms of low malignant potential and Grade 1 papillary carcinomas of the bladder, *Cancer* **95** (2002), 784–790.

[29] D. Ramos, S. Navarro, R. Villamón, M. Gil-Salom and A. Llombart-Bosch, Cytokeratin expression patterns in of low grade papillary urothelial neoplasms of the urinary bladder, *Cancer* **97** (2003), 1876–1883.

[30] H. Samaratunga, D.V. Makarov and J.I. Epstein, Comparison of WHO/IUSP and WHO classification of non-invasive papillary urothelial neoplasms for risk of progression, *Urology* **60** (2002), 315–319.

[31] G. Sauter, F. Algaba, M.B. Amin et al., Non-invasive urothelial tumours, in: *WHO Classification of Tumours. Tumours of the Urinary System and Male Genital Organs*, J.N. Eble, G. Sauter, J.I. Epstein and I.A. Sesterhenn, eds, IARC Press, Lyon, 2004, pp. 110–118.

[32] M. Scarpelli, R. Montironi, L.M. Tarquini, P.W. Hamilton, A. Lopez Beltran, J. Ranger-Moore and P.H. Bartels, Karyometry detects subvisual differences in chromatin organisation state between non-recurrent and recurrent papillary urothelial neoplasms of low malignant potential, *J. Clin. Pathol.* **57** (2004), 1201–1207.

[33] StataCorp, *Stata Statistical Software: Release 8.2*, Stata Corporation, College Station, TX, 2003.

[34] R. van Velthoven, M. Petein, W. Oosterlinck, T. De Wilde, J. Mattelaer, M. Hardeman, R. Kiss and C. Decaestecker, Identification by quantitative chromatin pattern analysis of patients at risk for recurrence of superficial transitional bladder carcinoma, *J. Urol.* **164** (2000), 2134–2137.

[35] T. Young, P.W. Verbeek and B. Mayall, Characterization of chromatin distributions in cell nuclei, *Cytometry* **7** (1986), 467–474.